iScience

CellPress
OPEN ACCESS

Article

Mitochondrial dysfunction, lipids metabolism, and amino acid biosynthesis are key pathways for COVID-19 recovery

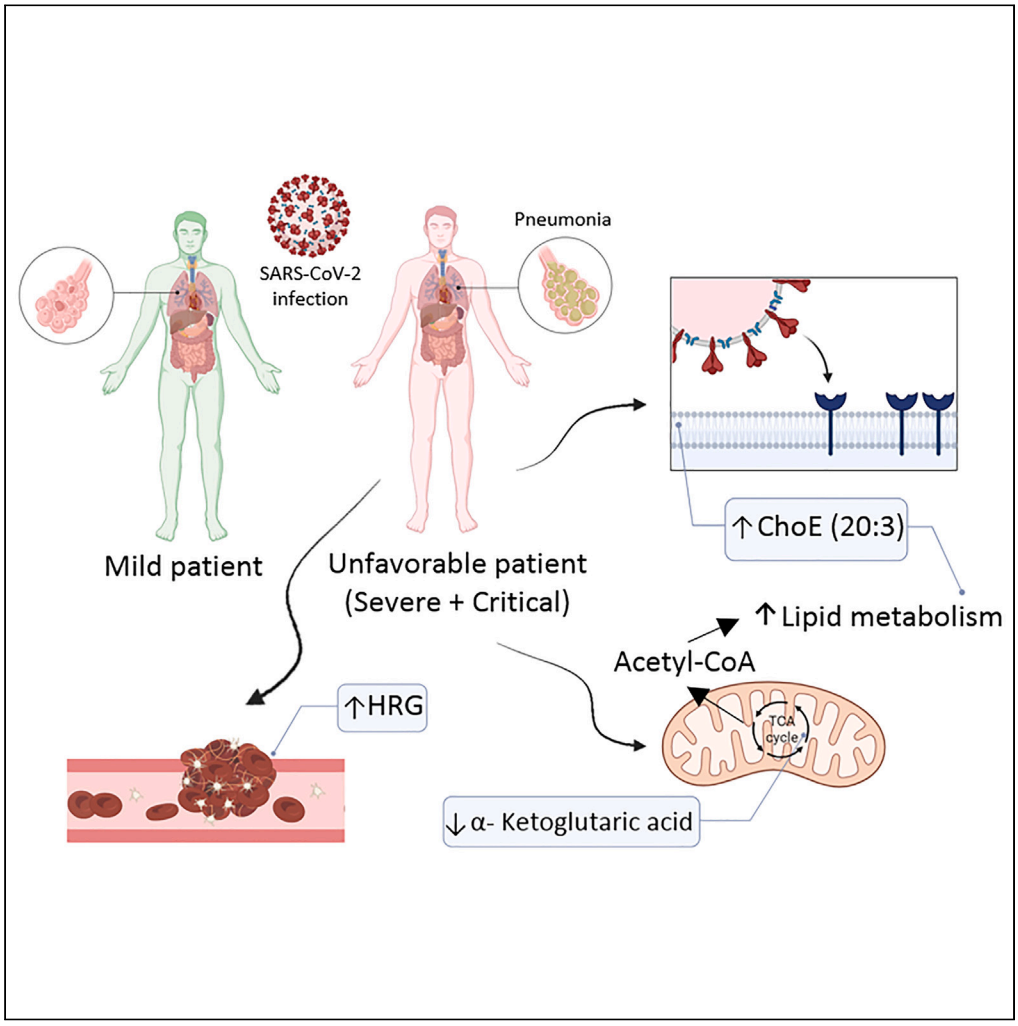

Alba Sánchez, Graciano García-Pardo, Fréderic Gómez-Bertomeu, ..., Anna Rull, Joaquim Peraire, for the COVIDOMICS Study Group

silvia.chafino@ciberinfec.es (S.C.)
anna.rull@iispv.cat (A.R.)

Highlights

Mitochondrial dysfunction is associated with the worst prognosis of COVID-19

Lipid metabolism, amino acid biosynthesis, and coagulation alterations with COVID-19

HRG, αKG, and ChoE (20:3) panel distinguished unfavorable from mild COVID-19 (AUC = 0.925)

Sánchez et al., iScience *26*, 107948
October 20, 2023
https://doi.org/10.1016/j.isci.2023.107948

iScience

CellPress
OPEN ACCESS

Article

Mitochondrial dysfunction, lipids metabolism, and amino acid biosynthesis are key pathways for COVID-19 recovery

Alba Sánchez,[1,2,9] Graciano García-Pardo,[1,2,3,4,9] Fréderic Gómez-Bertomeu,[1,2,3,4] Miguel López-Dupla,[1,2,3,4] Elisabet Foguet-Romero,[5] Maria José Buzón,[6,7] Benito Almirante,[3,6] Montserrat Olona,[1,2,3,4] Sonia Fernández-Veledo,[1,2,4,8] Francesc Vidal,[1,2,3,4] Silvia Chafino,[1,2,3,*] Anna Rull,[1,2,3,4,10,11,*] Joaquim Peraire,[1,2,3,4,10] and for the COVIDOMICS Study Group

SUMMARY

The metabolic alterations caused by SARS-CoV-2 infection reflect disease progression. To analyze molecules involved in these metabolic changes, a multiomics study was performed using plasma from 103 patients with different degrees of COVID-19 severity during the evolution of the infection. With the increased severity of COVID-19, changes in circulating proteomic, metabolomic, and lipidomic profiles increased. Notably, the group of severe and critical patients with high HRG and ChoE (20:3) and low alpha-ketoglutaric acid levels had a high chance of unfavorable disease evolution (AUC = 0.925). Consequently, patients with the worst prognosis presented alterations in the TCA cycle (mitochondrial dysfunction), lipid metabolism, amino acid biosynthesis, and coagulation. Our findings increase knowledge regarding how SARS-CoV-2 infection affects different metabolic pathways and help in understanding the future consequences of COVID-19 to identify potential therapeutic targets.

INTRODUCTION

COVID-19 is an infectious disease caused by a new type of virus from the Coronaviridae family, namely, severe acute respiratory syndrome coronavirus 2 (SARS-CoV-2).[1] People infected with SARS-CoV-2 present a great variety of symptoms from the most common, such as fever or cough, to pneumonia, respiratory failure, and even death in the worst cases.[2] The progression of SARS-CoV-2 infection depends on two essential steps: the interaction of the coronavirus spike protein with the host cell surface receptor and the activation of host cell mechanisms for viral replication and dissemination.[3] These events induce metabolic disturbances caused by viral infection. Under this scenario, multiomics studies on SARS-CoV-2 viral infection have greatly increased[4] and provided us with knowledge about the complexity of COVID-19 pathophysiology that can help medical units improve the diagnosis and prognosis of this disease. SARS-CoV-2, like other viruses, infects cells through the interaction of lipid membranes and reprograms different pathways for replication.[5] For instance, SARS-CoV-2 induces the expression of genes related to lipid metabolism, such as CD36, PPAR-γ, SREBP-1, and diacylglycerol acyltransferase-1, in monocytes.[6] Consequently, it is not surprising that a switch to fatty acid oxidation to fuel viral replication in patients with COVID-19 has been defined.[5] COVID-19 infection induces the production of several fatty acids, glycerophospholipids, and sphingolipids, which are required for the systemic inflammatory host response and energy metabolism and have been proposed as predictive biomarkers for COVID-19 severity.[1,3,7] As an example, butyric acid and L-phenylalanine, which are both increased in the serum of COVID-19 patients in comparison to healthy controls, are biomarkers related to inflammation, whereas 2-hydroxybutyric acid, which is increased in critical patients with lactic acidosis and ketoacidosis, is associated with lipid and carbohydrate metabolism.[8] On the other hand, the dysregulation of some plasma proteins during

[1]Institut Investigació Sanitària Pere Virgili (IISPV), Tarragona, Spain
[2]Hospital Universitari de Tarragona Joan XXIII (HJ23), Tarragona, Spain
[3]Centro de Investigación Biomédica en Red de Enfermedades Infecciosas (CIBERINFEC), Instituto de Salud Carlos III, Madrid, Spain
[4]Universitat Rovira i Virgili (URV), Tarragona, Spain
[5]Eurecat, Centre Tecnologic de Catalunya, Centre for Omic Sciences (Joint Unit Eurecat - Universitat Rovira i Virgili), Unique Scientific and Technical Infrastructure (ICTS), Reus, Spain
[6]Infectious Diseases Department, Hospital Universitari Vall d'Hebron, Barcelona, Spain
[7]Infectious Diseases Department, Vall d'Hebron Institute of Research (VHIR), Universitat Autònoma de Barcelona, (VHIR) Task Force COVID-19, Barcelona, Spain
[8]Centro de Investigación Biomédica en Red de Diabetes y Enfermedades Metabólicas Asociadas (CIBERDEM), Instituto de Salud Carlos III, Madrid, Spain
[9]These authors contributed equally
[10]These authors contributed equally
[11]Lead contact
*Correspondence: silvia.chafino@ciberinfec.es (S.C.), anna.rull@iispv.cat (A.R.)
https://doi.org/10.1016/j.isci.2023.107948

the development of COVID-19, such as HRG, FETUB, KNG1, LCAT, AHSG, and FN1, plays a key role in the survival of the most critically ill patients.[9] Of note, AHSG has been proposed as a good biomarker for detecting critical patients.[10]

Since most metabolomics studies of SARS-CoV-2 infection have been performed during the acute phase to find several biomarkers for diagnosis, much less is known about the different altered biomolecules associated with the progression of COVID-19 and which metabolic pathways are disturbed. Understanding how the infection biologically affects the organism is important for understanding the possible long-term consequences. We previously investigated circulating proteomic, metabolomic, and lipidomic profiles at the acute phase of infection to identify prognostic biomarkers for COVID-19 severity.[11] In the present study, we aimed to determine proteomic, metabolomic and lipidomic changes related to COVID-19 severity to provide insights into the long-term pathways affected by SARS-CoV-2 infection. This study investigated changes in serum biomolecules at 4–8 weeks after the acute phase of SARS-CoV-2 infection in patients with different COVID-19 severity.

RESULTS

Acute COVID-19 outcomes involve greater metabolic changes

The longitudinal cohort comprised 103 nonvaccinated patients with a COVID-19-positive diagnosis divided into three groups based on disease severity, namely, the mild, severe, and critical groups. The mild and severe groups were composed mainly of women (75% and 58.8%, respectively), whereas the critical group was formed mostly of men (60%). Range age was higher in the severe (50–75 years) and critical (50–67 years) groups than in the mild group (29–53 years) ($p < 0.001$). The most common symptoms in the three groups were fever and cough. Most critical patients presented dyspnea and asthenia (62.1% in both symptoms, $p < 0.001$) (Figure 1).

The evolution of proteomic, metabolomic and lipidomic profiles at 4–8 weeks (recovery phase) (Figure 1) was analyzed based on severity degree (Wilcoxon test). Data from the acute phase, which were previously published,[10] were considered for those patients with recovery phase sample availability to compare and normalize the data for this study. Specifically, in the mild group, a significant decrease in the relative abundance levels of 16 molecules was observed, with lipids being the predominant biomolecules (Figure 2A), and glycerolipid metabolism was one of the metabolomic pathways with greater incidence (Figure 2B; Table 1 and supplementary information 1). None of the biomolecules analyzed resulted in a significant increase in the recovery phase compared to the acute phase. In the severe group, the levels of 11 biomolecules, including citric acid, TGFb1 and ChoE (18:3), significantly increased, whereas 38 molecules decreased with a predominance of fatty acids and diacylglycerides, which were involved in the biosynthesis of unsaturated fatty acids (Figures 2C and 2D; Table 1). Regarding the group of critical patients, the relative abundance of five molecules was positively altered, and SFMBT2, GP5 and ChoE (18:0) specifically increased in this group of patients. On the other hand, the relative abundance levels of 63 biomolecules were significantly decreased during disease progression in critical patients. Valine, leucine, and serine, which are related to aminoacyl-tRNA biosynthesis, and glutamic acid and D-gluconic acid, which are associated with D-glutamine and D-glutamate metabolism and glyoxylate and dicarboxylate metabolism, were some of these biomolecules (Figures 2E and 2F; Table 1). Of note, five molecules were altered in all three severity groups, while seven were specific to the mild group, 21 to the severe group and 36 to the critical group (Figure 2G). Specifically, aspartic acid was the only metabolite whose levels decreased in all groups (Figures 2A, 2C, and 2E). In both the severe and critical groups, the levels of hippuric acid and ChoE (20:3) were significantly increased, whereas the levels of some metabolites, such as linoleic acid, phenylalanine or glutamic acid, triglycerides (TG 54:3, TG 52:2 and TG 50:1) and diglycerides (DG 36:3 and DG 36:4), were significantly decreased in the recovery phase compared to the acute phase (Figures 2C and 2E). These compounds, which were disturbed in both severe and critical patients, were implicated in different metabolic pathways, such as the linoleic acid, phenylalanine, glyoxylate and dicarboxylate pathways (Figures 2D and 2F; Table 1). Taken together, these results showed an association of COVID-19 severity with major changes in circulating proteomic, metabolomic and lipidomic profiles. Of interest in the mild group, only 16 biomolecules were significantly decreased, whereas 49 and 68 molecules were significantly disturbed in the severe and critical groups, respectively.

Similar multiomics profiling in severe and critical patients after 4–8 weeks of COVID-19 evolution

At 4–8 weeks of COVID-19 evolution (recovery phase), of a total of 239 proteins, 78 metabolites and 112 lipids (supplementary information 1), the Kruskal–Wallis test revealed significant 31 proteins, 51 metabolites and 31 lipids of which seven were found in the three groups of severity, 18 were significantly different between mild and severe, four between mild and critical and six between severe and critical (Figure S1A). A significant increase or decrease in relation to disease severity was represented in heatmaps by type of molecule and by severity group (Figure 3A). Although specific patterns were found for each group, some similarities were found in severe and critical patients who shared 29% and 37.3% of the proteomic and metabolomic profiles, respectively, compared to the mild group, in which compounds such as alpha-1B-glycoprotein (A1BG), carboxypeptidase N subunit 2 (CPN2), complement C1s subcomponent (C1S), alanine-glyoxylate aminotransferase (AGT), glutamic acid, 2-hydroxyisovaleric acid, alpha-ketoglutaric acid, oleic acid, PC 32:0 and DG 36:1 predominated (Figure 3A). Of note, a high presence of immunoglobulins [immunoglobulin heavy variable 3–72 (IGHV3-72), immunoglobulin kappa variable 4-1 (IGKV4-1), immunoglobulin heavy constant alpha 1 (IGHA1), immunoglobulin kappa constant (IGKC), immunoglobulin lambda-like polypeptide 5 (IGLL5), immunoglobulin heavy constant mu (IGHM), immunoglobulin heavy constant gamma 1 (IGHG1), immunoglobulin heavy constant gamma 4 (IGHG4) and immunoglobulin heavy constant gamma 2 (IGHG2)] as well as alanine, indole-3-propionic acid, indolelactic acid, valine, s-xylose, d-arabinose and most of the triacylglycerols (TGs) was observed in severe patients. On the other hand, the most prevalent biomolecules in critical patients were histidine-rich glycoprotein (HRG), clusterin (CLU), apolipoprotein F (APOF), benzoic acid, palmitic acid, methionine, sphingomyelin 43:1 (SM 43.1), diacylglycerol 40:4 (DG 40:4), cholesteryl ester 22:4 [ChoE (22:4)] and cholesteryl ester 18:0 [ChoE (18:0)],

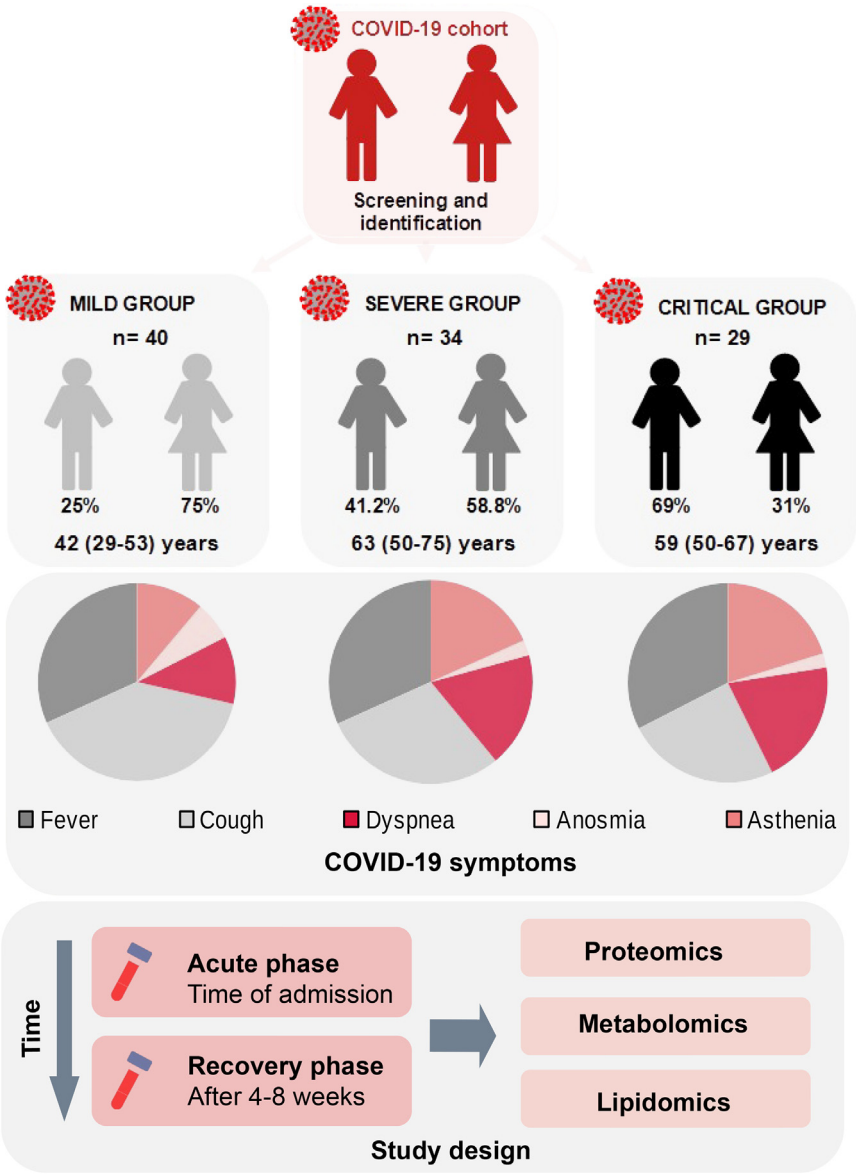

Figure 1. Study design, demographic and symptomatology data of the COVID-19 study cohort

The cohort for this longitudinal study comprised 103 nonvaccinated patients infected with SARS-CoV-2 classified based on disease severity into three groups: the mild, severe and critical groups. Demographic and symptomatology data were recorded at the time of admission. In every group, sex proportion (in percentage; %) and age range (median and 25th-75th interquartile range) are indicated. Blood sampling for multiomics analysis was performed at the time of admission (acute phase, data from previous study[10]) and after 4 to 8 weeks (recovery phase).

coinciding with their low prevalence in the other groups (Figure 3B). Interestingly, in critically ill patients, cholesterol compounds were strongly present in contrast with most phosphatidylcholines (PCs) and TGs, which were significantly decreased in this group (Figure 3A).

Regarding changes observed in the protein profile (Figures 3A and 3B), the proteins were functionally interconnected. Most of those proteins were significantly involved in the complement and coagulation cascades and lipoprotein particles, and more interestingly, four [HRG, fetuin-B (FETUB), heparin cofactor 2 (SERPIND), and plasminogen (PLG)] of them were further associated with COVID-19, thrombosis and anticoagulation pathways, and regulation of fibrinolysis ($p < 0.05$) (Figure 3B). Formation of fibrin clots (clotting cascade), serine-type endopeptidase inhibitor activity, hemostasis, retinoid cycle disease events, lipopolysaccharide receptor complex, toxic pneumonitis, hemolytic uremic syndrome and aortitis were other processes in which the significant proteins were involved ($p < 0.05$).

In relation to the enriched pathways in which metabolites and lipids related to COVID-19 severity were identified after 4–8 weeks of infection, D-glutamine and D-glutamate metabolism, butanoate metabolism, tricarboxylic acid (TCA) cycle, arginine biosynthesis and alanine, aspartate and glutamate metabolism predominated independently of severity, as shown in Figure 3C. Analyzing by groups, D-glutamine

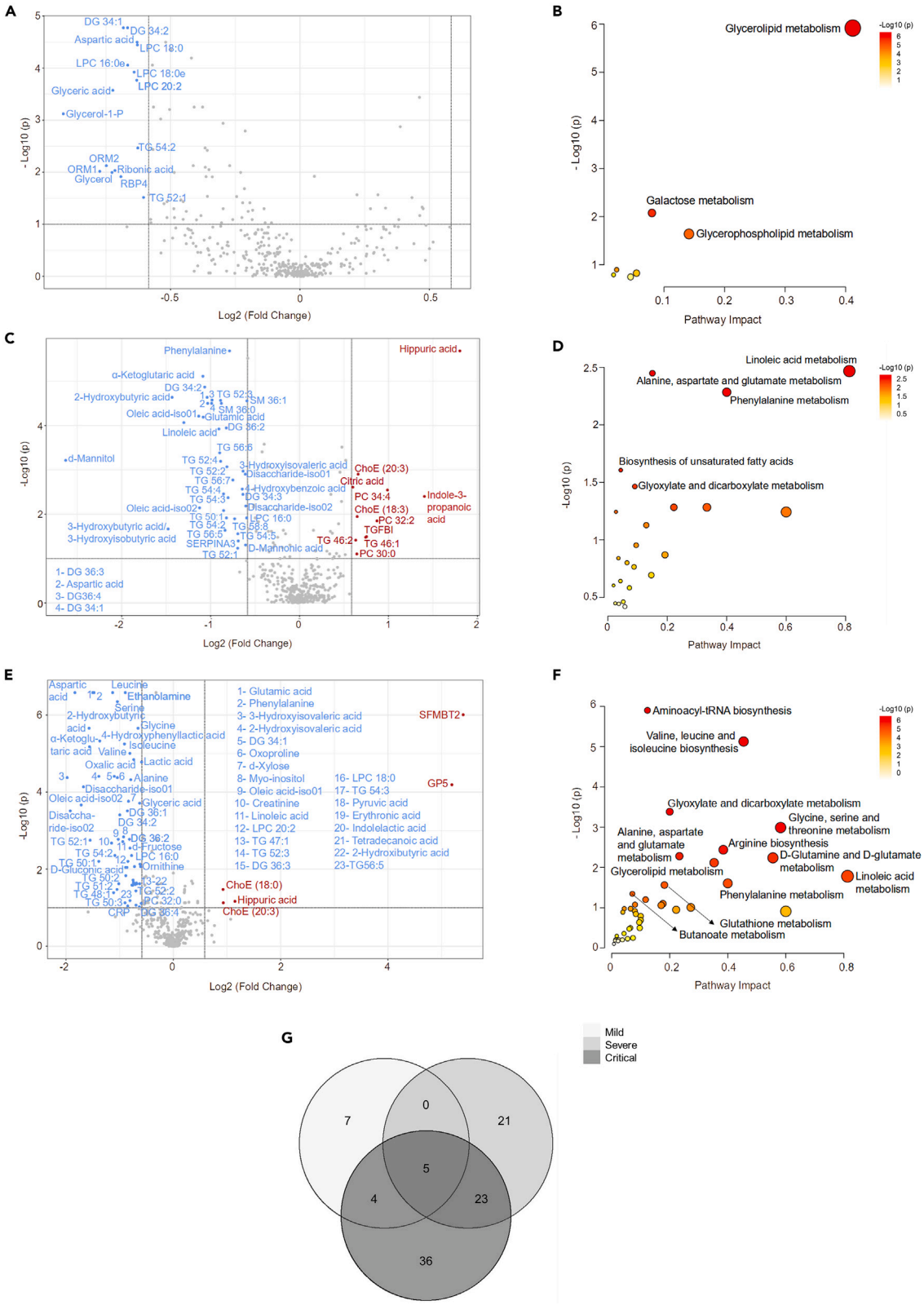
A
DG 34:1
DG 34:2
Aspartic acid
LPC 18:0
LPC 16:0e
LPC 18:0e
LPC 20:2
Glyceric acid
Glycerol-1-P
TG 54:2
ORM2
ORM1
Ribonic acid
Glycerol
RBP4
TG 52:1
- Log10 (p)
Log2 (Fold Change)
B
Glycerolipid metabolism
-Log10 (p)
Galactose metabolism
Glycerophospholipid metabolism
- Log10 (p)
Pathway Impact
C
Phenylalanine
Hippuric acid
α-Ketoglutaric acid
DG 34:2
2-Hydroxybutyric acid
SM 36:1
Oleic acid-iso01
Glutamic acid
Linoleic acid
DG 36:2
TG 56:6
d-Mannitol
TG 52:4
3-Hydroxyisovaleric acid
TG 52:2
Disaccharide-iso01
ChoE (20:3)
Citric acid
TG 56:7
TG 54:4
4-Hydroxybenzoic acid
PC 34:4
Indole-3-propanoic acid
TG 54:3
DG 34:3
Disaccharide-iso02
ChoE (18:3)
Oleic acid-iso02
LPC 16:0
PC 32:2
TG 50:1
TG 54:2
TG 58:8
TGFBI
3-Hydroxybutyric acid/
3-Hydroxyisobutyric acid
TG 56:5
TG 54:5
TG 46:2
TG 46:1
SERPINA3
D-Mannonic acid
PC 30:0
TG 52:1
1- DG 36:3
2- Aspartic acid
3- DG36:4
4- DG 34:1
-Log10 (p)
Log2 (Fold Change)
D
Linoleic acid metabolism
Alanine, aspartate and glutamate metabolism
Phenylalanine metabolism
-Log10 (p)
Biosynthesis of unsaturated fatty acids
Glyoxylate and dicarboxylate metabolism
-Log10 (p)
Pathway Impact
E
Aspartic acid
Leucine
Ethanolamine
Serine
2-Hydroxybutyric acid
Glycine
α-Ketoglutaric acid
4-Hydroxyphenyllactic acid
Isoleucine
Valine
Lactic acid
Oxalic acid
Alanine
Disaccharide-iso01
Oleic acid-iso02
Glyceric acid
Disaccharide-iso02
DG 36:1
DG 34:2
TG 52:1
DG 36:2
d-Fructose
TG 54:2
LPC 16:0
TG 50:1
Ornithine
D-Gluconic acid
TG 50:2
TG 52:2
TG 48:1
PC 32:0
TG 50:3
CRP
DG 36:4
1- Glutamic acid
2- Phenylalanine
3- 3-Hydroxyisovaleric acid
4- 2-Hydroxyisovaleric acid
5- DG 34:1
6- Oxoproline
7- d-Xylose
8- Myo-inositol
9- Oleic acid-iso01
10- Creatinine
11- Linoleic acid
12- LPC 20:2
13- TG 47:1
14- TG 52:3
15- DG 36:3
16- LPC 18:0
17- TG 54:3
18- Pyruvic acid
19- Erythronic acid
20- Indolelactic acid
21- Tetradecanoic acid
22- 2-Hydroxibutyric acid
23-TG56:5
SFMBT2
GP5
ChoE (18:0)
Hippuric acid
ChoE (20:3)
-Log10 (p)
Log2 (Fold Change)
F
Aminoacyl-tRNA biosynthesis
Valine, leucine and isoleucine biosynthesis
-Log10 (p)
Glyoxylate and dicarboxylate metabolism
Glycine, serine and threonine metabolism
Alanine, aspartate and glutamate metabolism
Arginine biosynthesis
D-Glutamine and D-glutamate metabolism
Glycerolipid metabolism
Linoleic acid metabolism
Phenylalanine metabolism
Glutathione metabolism
Butanoate metabolism
-Log10 (p)
Pathway Impact
G
Mild
Severe
Critical
7
0
21
5
4
23
36

Figure 2. Evolution of proteomic, metabolomic and lipidomic profiles of the COVID-19 cohort based on disease severity

(A–F) Volcano plot comparing proteomic, metabolomic and lipidomic profiles in the recovery phase from the acute phase in (A) mild, (C) severe and (E) critical individuals. Significantly ($p < 0.05$) upregulated molecules in COVID-19-positive patients are highlighted in red, and downregulated molecules are highlighted in blue. The log2-fold change in molecular levels is represented on the x-axis, and the -log10 Wilcoxon test p value is on the y axis. Abbreviations: TG: triglyceride; DG: diglyceride; LPC: lysophosphatidylcholine; SM: sphingomyelin and ChoE: cholesteryl ester. The bubble diagram shows the relevant metabolic pathways in which the molecule profiles have changed significantly considering all patients classified by severity: (B) mild, (D) severe and (F) critical individuals. Joint-pathway analysis sorted by pathway impact and -log10 greater than 0.1 (p value < 0.05) were further considered. The size of the bubbles shows the pathway impact value, and the color denotes the level of significance (from non-significant pathways in yellow to significant in red) by the mean of p values. Significant pathways were named in the bubble plot and p values and matched molecules are described in Table 1 and supplementary information 1.

(G) A Venn diagram indicates the number of compounds that were shared or not shared by mild, severe and critical groups. Different colors are corresponded to different severity groups.

and D-glutamate metabolism and butanoate metabolism pathways were the most predominant in the mild and severe patients (Figures S1B and S1C). However, in the critical group, selenocompound and propanoate metabolism, fatty acid elongation and fatty acid degradation were the predominant enriched pathways, suggesting that COVID-19 severity is related to more metabolomic changes (Figure S1D).

Overall, these findings suggested that severe and critical patients share minor differences in biochemical composition (similar proteomic and metabolomic profiles among groups, Figure 3A), but the implication of these differences in biological pathways is different (Figure S1), changing more in the critical group in the recovery phase.

HRG, alpha-ketoglutaric acid and ChoE (20:3) as multiomics-based biomarkers for unfavorable COVID-19 evolution

To identify key biomarkers for unfavorable progression of COVID-19, the severe and critical groups were grouped into the "unfavorable" group (hereinafter, the study groups were mild and unfavorable). In this way, metabolic pathways explaining how mild COVID-19 could become a more adverse diagnosis could be revealed.

In this longitudinal cohort with this new classification, the mild group was composed mainly of women (75%), whereas the unfavorable group comprised 54% men. Range age was higher in the unfavorable group (51–72 years) than in the mild group (28–53 years) ($p < 0.001$). Patients in the mild group had obesity (50%), hypertension (12.5%), dyslipidemia (12.5%) and cardiovascular problems (10%) before SARS-CoV-2 infection. In the case of patients in the unfavorable group, the most important previous comorbidities were obesity (63.5%) and hypertension (34.9%). Dyslipidemia (27%), diabetes mellitus (17.5%) and metabolic syndrome (14.3%) were also present in this group of patients, which reaffirmed that the unfavorable group presented a higher prevalence of comorbidities than the mild group. Moreover, the 65% of mild patients exercised regularly ($p = 0.022$) (Table 2).

Table 1. Significant metabolomic pathways involved in the evolution of COVID-19 infection

	MILD		SEVERE		CRITICAL	
Pathway name	Match	p value	Match	p value	Match	p value
Alanine, aspartate and glutamate metabolism	–	–	3/61	0.003	4/61	0.005
Aminoacyl-tRNA biosynthesis	–	–	–	–	8/74	1.257E-6
Arginine biosynthesis	–	–	–	–	3/27	0.003
Biosynthesis of unsaturated fatty acids	–	–	2/47	0.024	–	–
Butanoate metabolism	–	–	–	–	2/29	0.045
D-Glutamine and D-glutamate metabolism	–	–	–	–	2/10	0.005
Galactose metabolism	2/51	0.008	–	–	–	–
Glutathione metabolism	–	–	–	–	3/56	0.027
Glycerolipid metabolism	4/35	1.2063E-6	–	–	3/35	0.007
Glycerophospholipid metabolism	2/86	0.022	–	–	–	–
Glycine, serine and threonine metabolism	–	–	–	–	5/68	0.001
Glyoxylate and dicarboxylate metabolism	–	–	2/56	0.034	5/56	4.145E-4
Linoleic acid metabolism	–	–	2/17	0.003	2/17	0.016
Phenylalanine metabolism	–	–	2/21	0.005	2/21	0.024
Valine, leucine and isoleucine biosynthesis	–	–	–	–	4/12	7.470E-6

Profile of the number of matched molecules in relation to known compounds of each pathway and p value corresponding to each pathway impact from the joint-pathway analysis are indicated in mild, severe and critical groups. The specific molecules of each pathway are described in supplementary information 1.

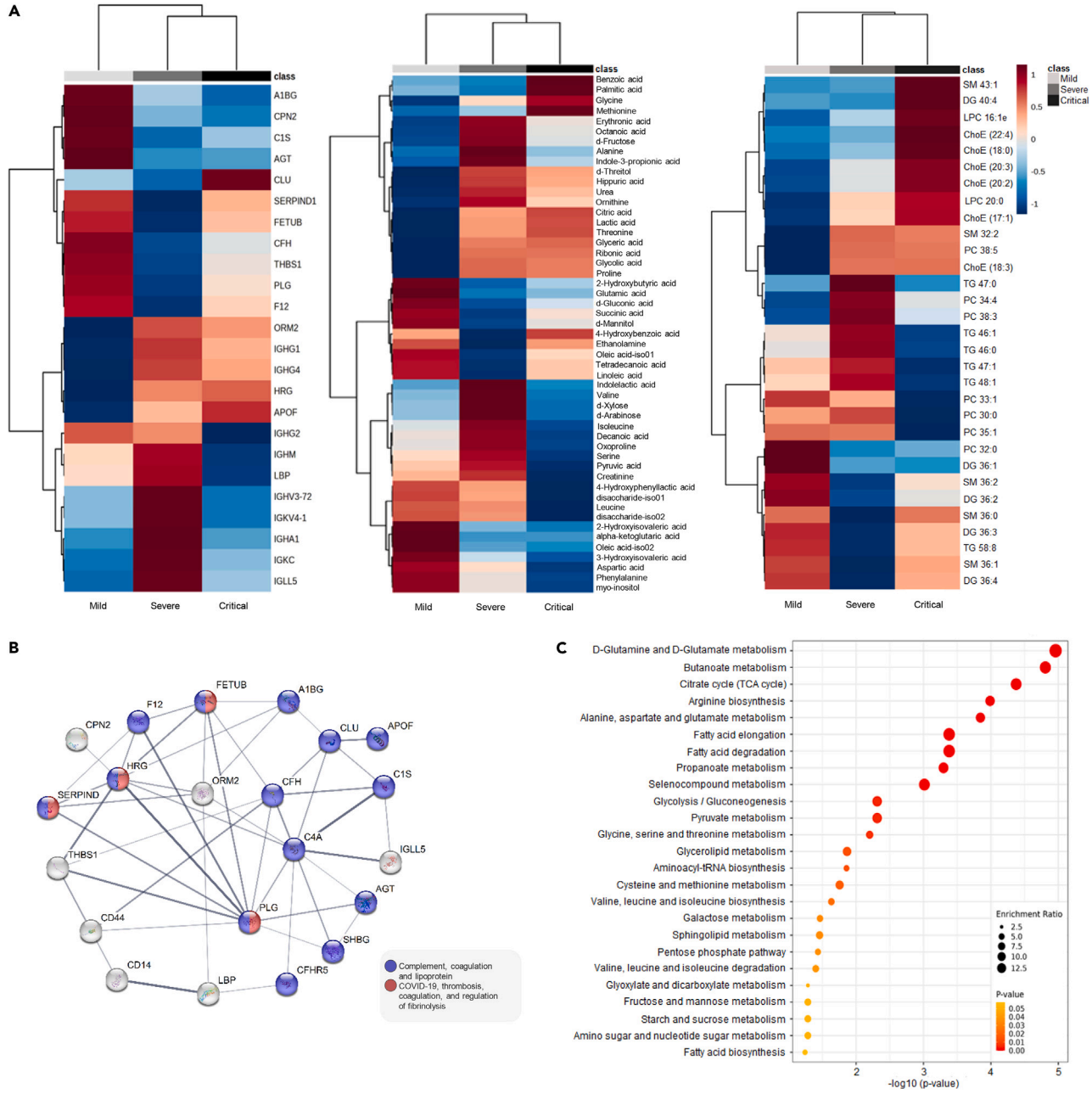

Figure 3. Distribution and implication of different biomolecules and pathways during the recovery phase in COVID-19 patients

(A) Heatmaps of proteomic, metabolomic and lipidomic (left to right) significant profiles by disease severity using MetaboAnalyst 5.0. The columns in each heatmap indicate the mild (left), severe (center) and critical (right) groups, and the color intensity shows the abundance of the compound in each group (increased in red and decreased in blue). Biomolecules with significant differences (p values <0.05) between groups were determined by the nonparametric Kruskal–Wallis test. Biomolecules with >50% missing values were removed.

(B) Network of significant proteins in COVID-19-infected patients using STRING 11.5. In violet: proteins involved in complement, regulation and lipoprotein; in red: proteins related to COVID-19, thrombosis, coagulation, and regulation of fibrinolysis. Significant proteins (p values <0.05) were determined by the nonparametric Kruskal–Wallis test.

(C) Enrichment analysis by Kyoto Encyclopedia of Genes and Genomes (KEGG) using MetaboAnalyst 5.0 of significant metabolites and lipids among COVID-19-infected patients. The gradient of color indicates the p value degree, with red being the most significant. Significant metabolites and lipids (p values <0.05) were determined by the nonparametric Kruskal–Wallis test.

Table 2. Demographic information from patients of the longitudinal cohort using the new classification criteria

Variables	Mild (n = 40)	Unfavorable (n = 63)	p value
Male	10 (25)	34 (54)	**<0.001**
Age (years)	42 (28–53)	60 (51–72)	**0.004**
Comorbidities			
Obesity	20 (50)	40 (63.5)	**0.04**
Metabolic syndrome	0 (0)	9 (14.3)	0.364
Diabetes mellitus (DM)	0 (0)	11 (17.5)	**0.005**
Hypertension (HTA)	5 (12.5)	22 (34.9)	**0.012**
Dyslipidemia (DLP)	5 (12.5)	17 (27)	0.800
Cardiovascular diseases (CVD)	4 (10)	6 (9.5)	0.937
Respiratory diseases (COPD)	2 (5)	0 (0)	0.730
Cancer	2 (5)	2 (3.2)	0.640
Lifestyle factors			
Exercise	26 (65)	24 (38.1)	**0.022**
Smoker	4 (10)	4 (6.3)	0.056
Habitual alcohol consumption	3 (7.5)	8 (12.7)	0.398

Data are presented as n (%) or median (25th-75th interquartile range).

First, a random forest analysis was performed. Figure 4A shows the top 15 significant proteins, metabolites and lipids that better differentiated the two groups. The top two biomolecules in each random forest analysis were selected as biomarker candidates: HRG and thrombospondin 1 (THBS1) (proteins), 2-hydroxyisovaleric acid and alpha-ketoglutaric acid (metabolites), phosphatidylcholine 32:0 (PC 32:0) and cholesteryl esters ChoE (20:3) (lipids). Of note, the compounds HRG and ChoE (20:3) were significantly higher in the unfavorable group, and THBS1, 2-hydroxyisovaleric acid, alpha-ketoglutaric acid and PC 32:0 were significantly higher in the mild group (Figure 4A). Interestingly, the HRG candidate was not only associated with the unfavorable group but also previously related to immune system processes and COVID-19 (Figure 3B). Metabolomic-based biomarker analysis by receiver operating characteristic (ROC) curves was performed individually for the six candidates mentioned above and represented by the type of molecule (Figure S2). Four of the biomarkers obtained good outcomes for the area under the curve (AUC) (AUC >0.65): alpha-ketoglutaric acid (AUC = 0.878; 95% CI = 0.818–0.939; p = 0.000), 2-hydroxyisovaleric acid (AUC = 0.805; 95% CI = 0.724–0.885; p = 0.000), ChoE (20:3) (AUC = 0.739; 95% CI = 0.644–0.834; p = 0.000) and HRG (AUC = 0.682; 95% CI = 0.569–0.796; p = 0.003) (Figure S2). The other two compounds, THBS1 and PC 32:0, were eliminated from the next analysis due to their low AUC results (THBS1: AUC = 0.349, 95% CI = 0.235–0.464, p = 0.015; PC 32:0: AUC = 0.373, 95% CI = 0.271–0.475, p = 0.020).

Then, the discriminatory power of selected biomarkers for differentiating mild and unfavorable groups was analyzed by binary logistic regression. The combination of the four selected biomarkers [HRG + alpha-ketoglutaric acid + 2-hydroxyisovaleric acid + ChoE (20:3) (Model 1)], rather than using each biomolecule individually, significantly increased the discriminatory power of these compounds (AUC = 0.924). Because the selected panel of four biomolecules included one protein, two metabolites and one lipid, we tested the prediction accuracy of using only one molecule representing each type of molecule (combinations of three different natural compounds). The best discriminatory power was obtained by the combination of HRG + alpha-ketoglutaric acid + ChoE (20:3) (AUC = 0.925; 95% CI = 0.872–0.979; p < 0.001; Model 2), in contrast to the combination of HRG + 2-hydroxyisovaleric acid + ChoE (20:3) (Model 3), which presented an AUC value of 0.785 (Figure 4B). Of note, the combination of the three selected biomolecules together showed the best discrimination between groups due to its high specificity and sensitivity rather than considering them individually. These biomarkers associated with specific COVID-19 unfavorable diagnoses could help to identify possible targeting COVID-19 progression-specific metabolic pathways.

Next, to analyze whether the levels of the biomarkers were affected by age (p = 0.004) and gender (p < 0.001) in the proposed panels, logistic regression models including these factors for mild and unfavorable patients were performed using the Model 1 and the Model 2 as they obtained the best AUC (Figure 4B). The Odds Ratio (OR) for age was 1.066 for both models (p = 0.027 and 0.029, respectively) and the OR for gender was 3.451 (p = 0.184) for Model 1 and 3.168 (p = 0.198) for Model 2, indicating that gender was not associated with proposed panels (Table 3). Therefore, age was the only significantly factor which contribute to the plasma molecule panels and for this reason, ROC curves of Model 1 [HRG + alpha-ketoglutaric acid + 2-hydroxyisovaleric acid + ChoE (20:3)] and Model 2 [HRG + alpha-ketoglutaric acid + ChoE (20:3)] were performed including age as factor. The best discriminatory power was obtained by the combination of age and Model 1 (AUC = 0.954; 95% CI = 0.913–0.995; p < 0.001) (Figure 4C) whereas the combination of age with Model 2 obtained AUC of 0.949 (95% CI = 0.904–0.994; p < 0.001) (Figure 4C). Moreover, the relation of comorbidities with the four main biomolecules proposed associated to unfavorable group were analyzed by the coefficient of point-biserial correlation (*pb*) and represented in a correlation matrix. The results confirmed that HRG, alpha-ketoglutaric acid and ChoE (20:3) were not affected by any previous comorbidities (Figure 4D). Hence, the age was a factor which improved the discriminatory power of plasma molecule panel to distinguish mild from unfavorable patients.

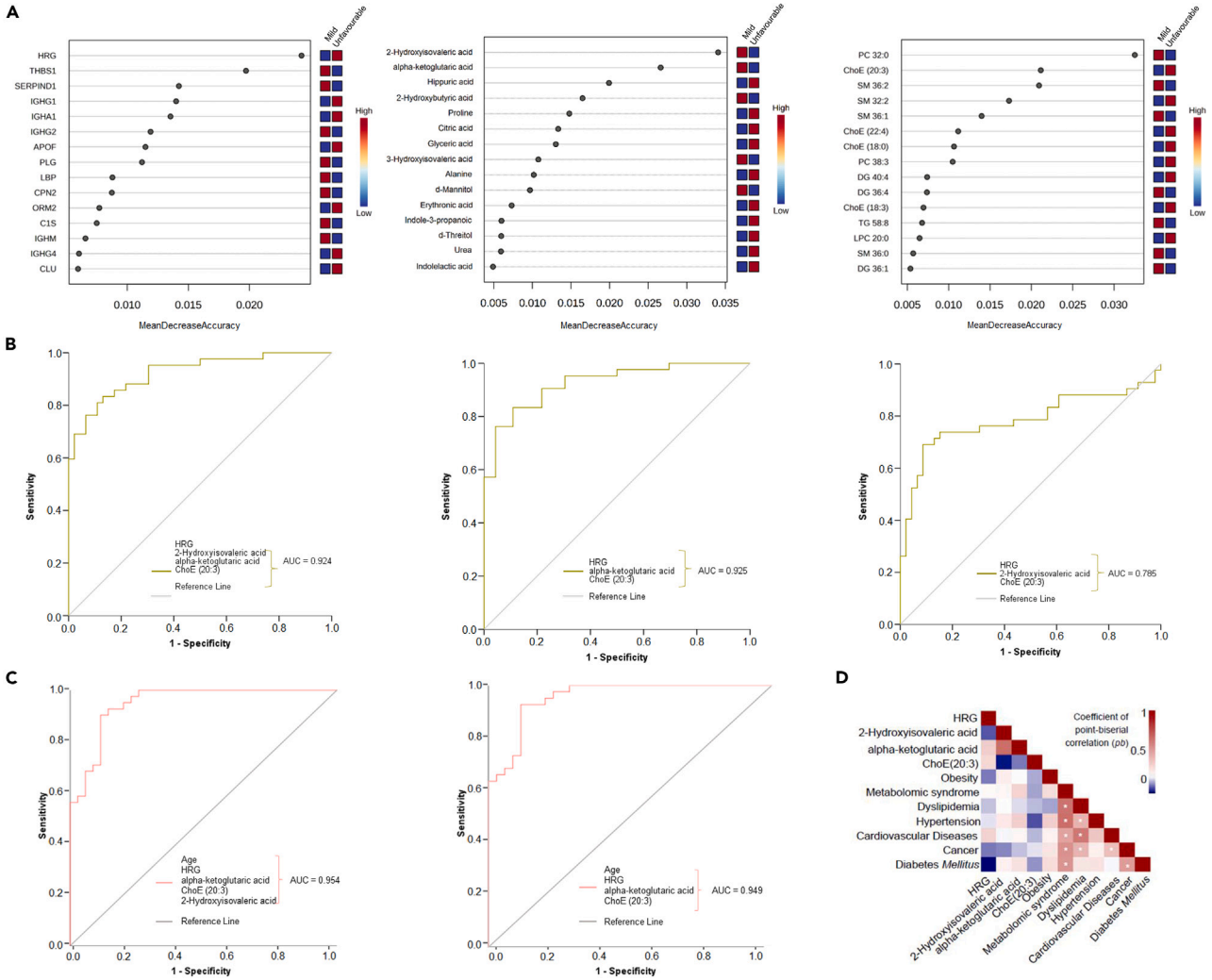

Figure 4. Biomarker analysis for distinguishing COVID-19 progression from mild to unfavorable

(A) Random forest of significant proteins, metabolites and lipids (left to right) in patients comparing mild and unfavorable disease outcomes by MetaboAnalyst 5.0. The intensity of colors indicates the significance of the compound in differentiating groups (high in red and low in blue).

(B) ROC curves of selected biomarkers for differentiating mild from unfavorable COVID-19 patients by binary logistic regression using IBM SPSS Statistics 21.0.

(C) ROC curves of Model 1 and Model 2 including age for differentiating mild from unfavorable COVID-19 patients by binary logistic regression using IBM SPSS Statistics 21.0.

(D) Heatmap showing the point-biserial correlation coefficient (*pb*) of pairwise comparison analyses between previous comorbidities with levels of selected biomarkers. The correlation matrix is color-coded according to the point-biserial correlation coefficient (−1:1, blue:red through white), and correlations with statistical significance are indicated with an asterisk as *p < 0.05.

DISCUSSION

COVID-19 has become a public health problem affecting ~700.0 million confirmed patients with high variability of symptoms such as fever or cough in mild patients to pneumonia and complicated dyspnea in critical patients.[12] Most patients present mild symptoms, whereas a small proportion of patients infected with SARS-CoV-19 progress to critical illness with multi-organ failure accompanied by metabolic disturbances.[13]

The study of the metabolic changes that underlie the evolution of COVID-19 infection generates knowledge for understanding this pandemic disease and consequently for identifying specific biomarkers to act early in COVID-19 diagnosis and treatment. Thus, this longitudinal study of nonvaccinated SARS-CoV-2-infected patients provides a comprehensive perspective on circulating proteomic, metabolomic and lipidomic signatures associated with different COVID-19 severity degrees, from mild to critical outcomes. Previously published data described fetuin-A, glutamic acid and ChoE (18:0) as key predictive biomarkers for distinguishing mild from critical patients in the acute phase of SARS-CoV-2 infection.[10] Interestingly, in this study of 103 patients from a previous cohort with well-characterized follow-up until the recovery phase, the TCA cycle, lipid metabolism and amino acid biosynthesis were the key pathways in good COVID-19 healing. In addition,

Table 3. Multivariable analysis of the associations of age and gender with COVID-19 severity

	Variables	Odds ratio	95% CI	p value
Model 1	Age	1.066	1.007–1.129	**0.027**
	Gender	3.451	0.555–21.443	0.184
Model 2	Age	1.066	1.007–1.129	**0.029**
	Gender	3.168	0.547–18.359	0.198

Model 1 was compound by HRG + alpha-ketoglutaric acid + 2-hydroxyisovaleric acid + ChoE (20:3) and the Model 2 was formed by the combination of HRG + alpha-ketoglutaric acid + ChoE (20:3).

analyzing the changes between two time points (baseline and after 4–8 weeks), the proteome, metabolome and lipidome after 4–8 weeks were still different from the acute phase of COVID-19.[10] The major number of changes was found in critical group with 68 molecules, followed by the severe group with 49 and finally by the mild group with only 16 decreased biomolecules found in relation to baseline. Surprisingly, most of the up-regulated changes were observed in the severe group with 11 biomolecules and not in the critical group (5 increased biomolecules), probably because this comparison evaluated changes between the acute and recovery phase. This result indicates that the high levels of most biomolecules in the critical group did not vary along this period of time during infection and suggests that the up-regulation of the most biomolecules could have occurred during the acute phase as reported by some studies.[14–16] Moreover, several studies reported that during the acute phase, excessive release of cytokines and other inflammatory molecules can lead to multi-organ dysfunction or even death[17,18] and these consequences were reflected in changes in multiomics profiles during the recovery phase, where severity has been associated with increased alterations in pathways and molecules, indicating the tissue damage degree and the state of the immune system. Of note, in the recovery phase, fatty biosynthesis and elongation predominated together with butanoate and selenocompound metabolisms in the case of severe and critical groups, whereas synthesis of amino acids such as arginine, alanine and glutamate, together with an activation of the TCA cycle (Figure S1) probably by glutaminolysis[19] producing high levels of alpha-ketoglutaric acid, which was found in our study to be highly present in the mild group (Figure 3A). These results indicate that a good recovery is characterized by a predominance of anabolic processes as indicated by some studies,[20] while over-activation of the TCA cycle could end up breaking the cycle, worsening cellular function, and producing a poor recovery.[21]

Regarding the proteomic signature related to an unfavorable COVID-19 outcome, in the recovery phase, most of the significant molecules detected were related to complement function and coagulation along with the high presence of different immunoglobulins as reported in other studies.[4,15,22] In particularly in our study, a significant increase in the circulating relative abundance of HRG was found in severe and critical patients compared to the mild patients, reaffirming its importance in several metabolic functions.[9] In agreement, Nishibori M. emphasized the decrease in plasma HRG levels at early phases of the disease to be used as a biomarker to distinguish between mild and severe cases.[23] HRG is produced primarily by the liver and secreted into circulation, where it regulates many processes, such as coagulation and fibrinolysis.[24] It has been reported that HRG can bind to heparin, the main anticoagulant, preventing the activation of coagulation factors and therefore triggering the formation of blood clots (Figure 5A).[25] Remarkably, 50% of patients with severe COVID-19 showed coagulopathy problems associated with high levels of D-dimer protein.[26] And more recently, an association of thromboembolic complications with Long COVID was described, by mechanisms such as persistent inflammation, coagulation abnormalities, endothelial damage and dysfunction.[27] Other functions of HRG are host defense, pathogen clearance, angiogenesis, dead cell clearance and tumor growth, which could be related to a protective effect of the organism against damage induced by SARS-CoV-2 infection.[23] Published data suggest that the changes in the plasma levels of HRG, especially in severe patients with COVID-19, are associated with its role in preventing the excessive activation of neutrophils and endothelial cells. In the case of neutrophils, HRG maintains a quiescent state and low production of reactive oxygen species (ROS). Regarding epithelial cells (ECs), HRG inhibits the release of the cytokine named high-mobility group box-1 (HMGB1) and consequently suppresses the inflammatory responses induced by HMGB1.[28,29] In addition, HRG maintains the integrity of ECs by inhibiting the reorganization of the cytoskeleton and regulating E-cadherin levels (Figure 5A).[18,19] Thus, HRG could be considered as a possible therapeutic target as an anti-thrombotic and regulator of neutrophil over-activation.

The levels of alpha-ketoglutaric acid, a common intermediate molecule of the tricarboxylic acid (TCA) cycle, decreased during the progression of COVID-19, reaching high levels in the mild group compared to the unfavorable group. Previously published data described increased circulating alpha-ketoglutaric acid concentrations in critical patients during the acute phase directly related to increased glutamic acid relative abundance in plasma.[10,30] Concretely, in the acute phase, an increase in the circulating relative abundance of glutamic acid was determined to be a key predictive biomarker for distinguishing mild from critically ill patients.[31] Glutamic acid, which is synthesized from alpha-ketoglutaric acid[32] is a non-essential amino acid with a key role in the TCA cycle, gluconeogenesis and amino acid metabolism and hence acts as an oxidative stress and energy homeostasis controller under stress conditions. Moreover, macrophages and monocytes use glutamic acid for their proper function as antioxidant defenders through the glutathione synthesis pathway.[33] High levels of alpha-ketoglutaric acid inhibit SARS-CoV-2 replication in the human monocytic U937 cell line[34] and are associated with anti-inflammatory and anti-thrombotic roles. Of note, supplementary dietary alpha-ketoglutaric acid reduced clot formation, leukocyte accumulation and apoptotic tissue damage in the lungs of infected mice.[35] For this reason, alpha-ketoglutaric acid may be a good dietary strategy to prevent thrombosis and inflammation in patients with COVID-19, as it happened with other dietary supplements such as vitamin D or C which improve the recovery during SARS-CoV-2 infection.[35,36] Thus, in agreement with all these data, we found a decreased relative abundance of glutamic acid and

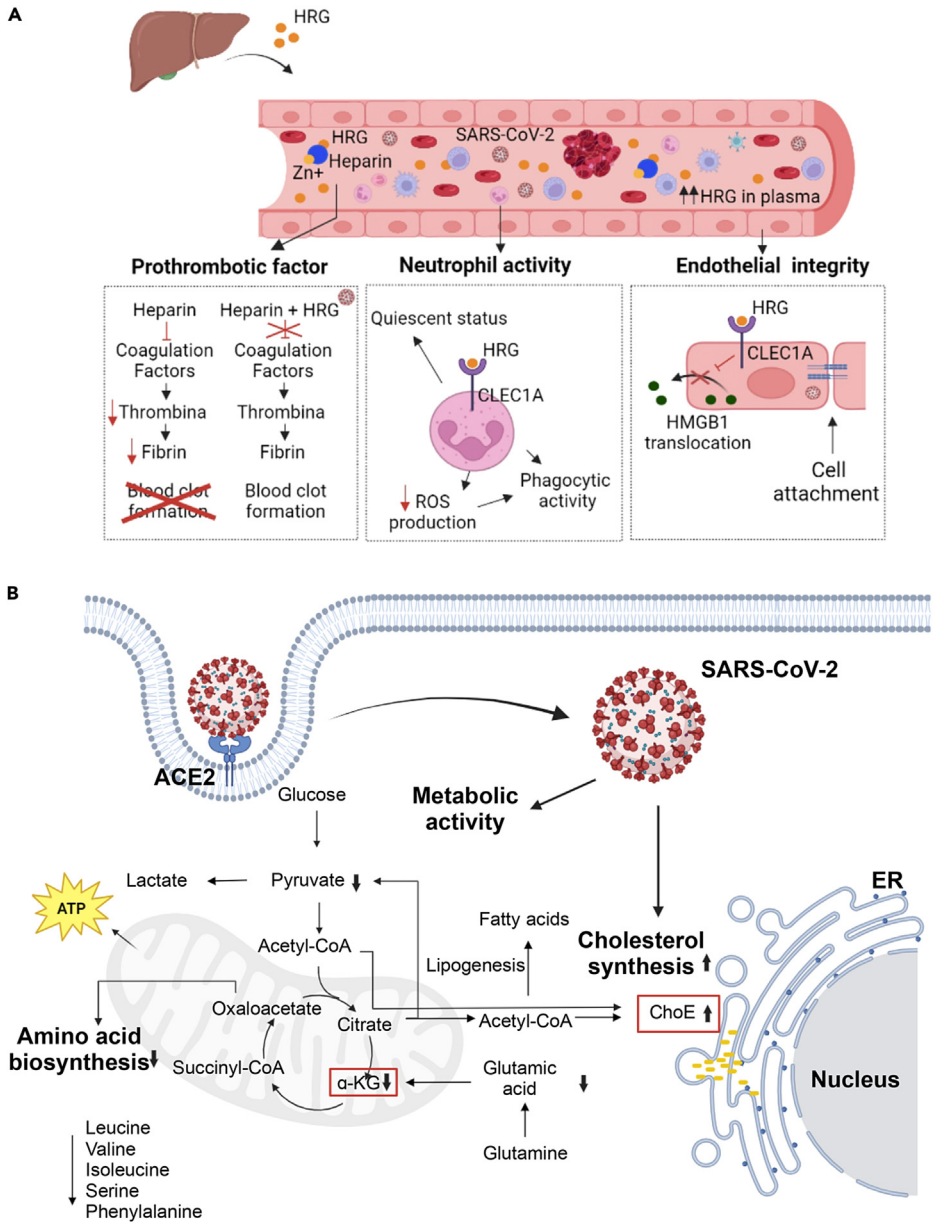

Figure 5. Molecular functions and metabolic pathways related to HRG, alpha-ketoglutaric acid and ChoE (20:3) biomarkers based on COVID-19 severity

(A) HRG is synthesized in the liver and secreted into the bloodstream, where it interacts with several cell types and performs different functions. In SARS-CoV-2 infection, the prothrombotic factor HRG binds to heparin, preventing the interaction between coagulation factors and heparin and triggering blood clot formation. In neutrophils, HRG binds to its receptor, CLEL1A, which maintains the quiescent status and low production of ROS to promote phagocytic activity, and in epithelial cells, the activation of CLEL1A inhibits the translocation of the cytokine HMGB1 to the extracellular matrix and promotes cell attachment by regulating E-cadherin levels.

(B) In patients with severe COVID-19, the TCA cycle is altered by low levels of alpha-ketoglutaric acid due to low levels of its precursor, glutamic acid. Moreover, ChoE levels are increased through the increased activity of cholesterol synthesis. Finally, a reduction in the synthesis of amino acids such as leucine or serine, among others, is observed. Yellow dots correspond to cholesterol particles.

alpha-ketoglutaric acid in patients with the most unfavorable COVID-19 outcomes after 4 to 8 weeks of SARS-CoV-2 infection. Consequently, a worse progression of COVID-19 disease could be directly related to mitochondrial dysfunction, hypoxia, and tissue damage through the reduction of TCA cycle activation (Figure 5B).[37] Hence a possible therapy based on the administration of pharmacological modulators of mitochondrial function was suggested as a potential treatment for COVID-19 to improve patient recovery. In addition, mitochondrial dysfunction has already been described as one of the mechanisms involved in Long COVID[27] and for that, this new therapy could also be effective in Long

COVID, using compounds such as mitochondria-targeted antioxidants that inhibit inflammation and oxidative stress and thus prevent organ dysfunction.[38,39] Moreover, a significant reduction in glutamine, which is an arginine precursor and a derivative of glutamic acid implicated in aminoacyl-tRNA biosynthesis, was also previously described in critical COVID-19 patients.[40] Thus, it could be postulated that aminoacyl-tRNA biosynthesis has an important role in SARS-CoV-2 infection due to its role in immunity regulation against viral infection apart from its canonical function in protein synthesis.[41] Some studies have shown that aminoacyl-tRNA synthetase and the multisynthetase complex (MSC) have a non-enzymatic function after infection, such as replication or entry into the host cell. Additionally, aminoacyl-transfer RNA synthetase-interacting multifunctional protein (AIMP1 or p43), one of the MSC members, can be secreted from macrophages and monocytes to act as an active proinflammatory cytokine and innate immune response stimulator.[42] The other metabolite, 2-hydroxyisovaleric acid, also known as 2-hydroxy-3-methylbutyric acid, is a valine derivative and originates primarily from the metabolism of valine, leucine, and isoleucine and ketogenesis.[43] Thus, it was not surprising that not only the relative abundance of 2-hydroxyisovaleric acid but also valine, leucine and isoleucine levels were significantly decreased during the disease course in critical patients, while in mild and severe patients, they did not undergo any changes. Accordingly, low levels of 2-hydroxyisovaleric acid, which were detected in the acute phase of disease in critical COVID-19 patients, have been proven not to be restored in the first or second month of the recovery phase.[7] Moreover, consistent with our results, previous data also proposed 2-hydroxyisovaleric acid as a candidate biomarker of the severity of COVID-19.[44]

The lipidomic profile in critically ill patients was significantly disturbed in the specific content of cholesterol compounds compared to those of mild and severe patients. In the recovery phase of COVID-19 disease, cholesteryl esters (ChoEs) were significantly increased in critical patients in contrast with most TGs and phosphatidylcholines (PCs), which were significantly increased in mild and severe patients as previously reported.[45,46] Of note, and similar to those previously observed with the relative abundance of alpha-ketoglutaric and glutamic acid, the circulating signatures of both ChoEs and TGs were the opposite in the acute phase of critical patients; there was a significant ChoE decrease but a significant increase in the relative abundance of TGs.[10] For viral entry to be successful, it is important to highlight the role of the host cell membrane composition, where the virus can enter by plasma membrane fusion or endocytosis.[47] In this regard, cholesterol has a fundamental role in regulating the entry of the virus into the host cell by promoting membrane fusion, besides in viral translation/replication and immune activation (Figure 5B). In this regard, cholesterol has a fundamental role in regulating the entry of the virus into the host cell by promoting membrane fusion, in addition to viral translation/replication and immune activation (Figure 5B). The viral fusion protein and the viral spike protein of SARS-CoV-2 require interaction with cholesterol to enter the host cell.[48] Specifically, elevated membrane cholesterol levels improve the efficiency of SARS-CoV-2 to enter and infect the host cell because this compound increases the number of entry sites and the number of angiotensin-converting enzyme 2 (ACE2) receptors in the membrane.[49] In addition, the virus can hijack cholesterol metabolism for its assembly, maturation, and release of viral particles.[50] Thus, cholesterol is a key factor in SARS-CoV-2 infection and in COVID-19 disease evolution, and some lipid species are potential biomarkers for COVID-19 severity and targets for treatment to prevent the entry of the virus into the host cell and its subsequent translation and replication. Specifically, ChoE (20:3) has been proposed as a healing biomarker for the recovery phase, whereas our preliminary study[10] reported ChoE (18:0) as a predictive biomarker for distinguishing mild from critical patients in the acute phase. Accordingly, other authors proposed monitoring lipid metabolism and low cholesterol therapy in patients with COVID-19.[51] Of interest, despite both ChoEs being increased along the disease course in critical patients (Figure 2E), we observed a change in the predominance of cholesterol type depending on the acute or recovery phase; therefore, further studies of specific cholesterol compounds would provide a greater understanding of the pathogenesis of SARS-CoV-2 infection. Interestingly, lipid metabolism alterations in the context of Long COVID were described as a risk factor for unfavorable outcomes, which could be modulate by metabolic interventions and diets as a possible therapy for improving symptoms of Long COVID.[52]

Finally, the best-proposed multiomics biomarkers associated with the COVID-19 recovery phase were HRG, alpha-ketoglutaric acid, and ChoE (20:3) because it is the best combination with the lowest number of compounds. However, age is a factor that directly influences the levels of these compounds. Many studies have linked age to a worse recovery from SARS-CoV-2 infection, so it is a factor to be considered when assessing the progression of the infection.[53,54] By contrast, any previous comorbidity did not affect. In conclusion, these biomolecules related to COVID-19 severity are associated with specific metabolic pathways, such as mitochondrial dysfunction, metabolism of lipids, amino acid biosynthesis, and the coagulation process. Knowledge of the molecular pathways altered due to viral infection that remain disturbed beyond the acute phase may help not only to understand the healing differences among SARS-CoV-2-infected subjects during the progression of COVID-19 but also to understand and anticipate the appearance of future pathologies derived from SARS-CoV-2 infection, such as long COVID. It would be of great interest to investigate the role of these molecules and molecular pathways to improve or create new treatments for emerging pandemic infections and for that, further studies would be needed to better understand the specific molecular mechanisms underlying these pathways.

Limitations of the study

Patients in this cohort were a representative, well-characterized group of patients with COVID-19 positivity from the first to third waves of SARS-CoV-2 infection in which experimental design the control group was considered the mild group of COVID-19 severity rather than a group of non-infected SARS-CoV-2 patients, according to the main objective of the study. The effect of different variants of SARS-CoV-2 has not been considered due to a lack of specific information; the small sample size impeded a more robust subgroup analysis and the applicability of the proposed panel of biomarkers is not immediate in clinical diagnosis. The present work identified various metabolic pathways, but it does not provide detailed mechanistic explanations for how SARS-CoV-2 infection specifically affects the different molecular pathways. One or two experiments at the cellular or animal level could be necessary to prove the significance of the target molecules. The dietary habits

and intake of the patients could affect the metabolic profiles in the different groups, and they were not possibly controlled in this study because the sampling was performed when the patients arrived at the hospital during the COVID-19 health crisis. Finally, it would be interesting to investigate the role of these molecules and molecular pathways related to different symptomatology of Long COVID-19.

CONSORTIA

The COVIDOMICS Study Group from Hospital Universitari Joan XXIII/IISPV/URV is composed of the following investigators who should be considered contributors to the paper: Verónica Alba, Montserrat Vargas, Anna Martí, Consuelo Viladés, Marina Flores, Lluïsa Guillem Tió, Beatriz Villar, Maria Teresa Mestre, Teresa Auguet, Laia Bertrán, Carmen Aguilar, José Antonio Porras, Sergi Veloso, Ajla Alibalic, David Riesco, Mónica Real, Jessica Binetti, Judit Poblet, Mercé Sirisi, Gaspar Dalmau, Vanessa Gázquez, Esther Rodriguez, Antonia Garcia, Esther Picó, Cristina Gutiérrez, Gemma Recio-Comí, Carla Martin-Grau, Teresa Sans, Carlos Chiapella, Pilar Carbajo, Mireia Cramp, Carme Bes, Rosalia Bote, Nuria Alba, Blanca Rosich, Cristina Varillas, Catherine Cabrejo, Júlia Vidal-González, Rosaura Reig, Llorenç Mairal, Jesús Esteve Ferrán, Neus Camañes, Angela Cortés and Rafael Gracia.

STAR★METHODS

Detailed methods are provided in the online version of this paper and include the following:

- KEY RESOURCES TABLE
- RESOURCE AVAILABILITY
  - Lead contact
  - Materials availability
  - Data and code availability
- EXPERIMENTAL MODEL AND SUBJECT DETAILS
  - Study participants and data collection
  - Ethics
- METHOD DETAILS
  - Sample recruitment
  - Proteomic analysis
  - Metabolomic analysis
  - Lipidomic analysis
- QUANTIFICATION AND STATISTICAL ANALYSIS
  - Statistical analysis

SUPPLEMENTAL INFORMATION

Supplemental information can be found online at https://doi.org/10.1016/j.isci.2023.107948.

ACKNOWLEDGMENTS

This work has been developed in the framework of the COVIDOMICS' project supported by Direcció General de Recerca i Innovació en Salut (DGRIS), Departament de Salut, Generalitat de Catalunya (PoC-6-17 and PoC1-5). The research was also supported by the Programa de Suport als Grups de Recerca AGAUR (2021SGR01404), the SPANISH AIDS Research Network [RD16/0025/0006]-ISCIII-FEDER (Spain) and the CIBER -Consorcio Centro de Investigación Biomédica en Red- (CB21/13/00020 and CB07/08/0012), Instituto de Salud Carlos III, Ministerio de Ciencia e Innovación and Unión Europea – NextGenerationEU. FV is supported by grants from the Programa de Intensificación de Investigadores (INT20/00031)-ISCIII and by "Premi a la Trajectòria Investigadora dels Hospitals de l'ICS 2018". AR is supported by a grant from IISPV through the project "2019/IISPV/05" (Boosting Young Talent), by GeSIDA through the "III Premio para Jóvenes Investigadores 2019" and by the Instituto de Salud Carlos III (ISCIII) under grant agreement "CP19/00146" through the Miguel Servet Program. Finally, this study would not have been possible without the generous collaboration of all the patients and their families and medical and nursing staff who have taken part in the project. We particularly acknowledge the collaboration of the Departments of Preventive Medicine and Epidemiology, Internal Medicine, Critical Care, Emergency, Occupational Health, Laboratory Medicine and Molecular Biology, and BioBank-IISPV (B.0000853 + B.0000854) integrated into the Spanish National Biobanks Platform (PT20/00197), CERCA Program (Generalitat de Catalunya) and IISPV, for their collaboration.

AUTHOR CONTRIBUTIONS

S.C.H., A.R., and J.P. had full access to the data in the study and take responsibility for the integrity of the data and the accuracy of the data analysis. Concept and design, S.C.H., A.R., J.P., and F.V.; acquisition, analysis, or interpretation of data, F.G-B., M.L-D., M.J.B., B.A., and M.O.; drafting of the manuscript, A.S., G.G-P., S.F-V., and S.C.H.; critical revision of the manuscript for important intellectual content, F.V., M.J.B., B.A., A.R., and J.P.; statistical analysis, A.S. and S.C.H.; funding acquisition, A.R. and F.V.; administrative, technical, or material support, E.F-R.; supervision A.R., J.P., and F.V.

DECLARATION OF INTERESTS

The authors declare no competing interests.

INCLUSION AND DIVERSITY

We support inclusive, diverse, and equitable conduct of research.

Received: May 8, 2023
Revised: August 29, 2023
Accepted: September 14, 2023
Published: September 19, 2023

REFERENCES

1. Meo, S.A., Alhowikan, A.M., Al-Khlaiwi, T., Meo, I.M., Halepoto, D.M., Iqbal, M., Usmani, A.M., Hajjar, W., and Ahmed, N. (2020). Novel coronavirus 2019-nCoV: prevalence, biological and clinical characteristics comparison with SARS-CoV and MERS-CoV. Eur. Rev. Med. Pharmacol. Sci. *24*, 2012–2019.
2. He, X., Cheng, X., Feng, X., Wan, H., Chen, S., and Xiong, M. (2020). Clinical Symptom Differences Between Mild and Severe COVID-19 Patients in China: A Meta-Analysis. Front. Public Health *8*, 561264. https://doi.org/10.3389/fpubh.2020.561264.
3. Mussap, M., and Fanos, V. (2021). Could metabolomics drive the fate of COVID-19 pandemic? A narrative review on lights and shadows. Clin. Chem. Lab. Med. *59*, 1891–1905. https://doi.org/10.1515/cclm-2021-0414.
4. Shen, B., Yi, X., Sun, Y., Bi, X., Du, J., Zhang, C., Quan, S., Zhang, F., Sun, R., Qian, L., et al. (2020). Proteomic and Metabolomic Characterization of COVID-19 Patient Sera. Cell *182*, 59–72.e15. https://doi.org/10.1016/j.cell.2020.05.032.
5. Bruzzone, C., Bizkarguenaga, M., Gil-Redondo, R., Diercks, T., Arana, E., García de Vicuña, A., Seco, M., Bosch, A., Palazón, A., San Juan, I., et al. (2020). SARS-CoV-2 Infection Dysregulates the Metabolomic and Lipidomic Profiles of Serum. iScience *23*, 101645. https://doi.org/10.1016/j.isci.2020.101645.
6. Dias, S.S.G., Soares, V.C., Ferreira, A.C., Sacramento, C.Q., Fintelman-Rodrigues, N., Temerozo, J.R., Teixeira, L., Nunes da Silva, M.A., Barreto, E., Mattos, M., et al. (2020). Lipid droplets fuel SARS-CoV-2 replication and production of inflammatory mediators. PLoS Pathog. *16*, e1009127. https://doi.org/10.1371/journal.ppat.1009127.
7. Shi, D., Yan, R., Lv, L., Jiang, H., Lu, Y., Sheng, J., Xie, J., Wu, W., Xia, J., Xu, K., et al. (2021). The serum metabolome of COVID-19 patients is distinctive and predictive. Metabolism *118*, 154739. https://doi.org/10.1016/j.metabol.2021.154739.
8. Cobb, J., Eckhart, A., Motsinger-Reif, A., Carr, B., Groop, L., and Ferrannini, E. (2016). α-Hydroxybutyric Acid Is a Selective Metabolite Biomarker of Impaired Glucose Tolerance. Diabetes Care *39*, 988–995. https://doi.org/10.2337/dc15-2752.
9. Völlmy, F., van den Toorn, H., Zenezini Chiozzi, R., Zucchetti, O., Papi, A., Volta, C.A., Marracino, L., Vieceli Dalla Sega, F., Fortini, F., Demichev, V., et al. (2021). A serum proteome signature to predict mortality in severe COVID-19 patients. Life Sci. Alliance *4*, e202101099. https://doi.org/10.26508/lsa.202101099.
10. Reverté, L., Yeregui, E., Olona, M., Gutiérrez-Valencia, A., Buzón, M.J., Martí, A., Gómez-Bertomeu, F., Auguet, T., López-Cortés, L.F., Burgos, J., et al. (2022). Fetuin-A, inter-α-trypsin inhibitor, glutamic acid and ChoE (18:0) are key biomarkers in a panel distinguishing mild from critical coronavirus disease 2019 outcomes. Clin. Transl. Med. *12*, e704. https://doi.org/10.1002/ctm2.704.
11. Wang, G.-Q., Zhao, L., Wang, X., Jiao, Y.-M., and Wang, F.-S. (2021). Diagnosis and Treatment Protocol for COVID-19 Patients (Tentative 8th Edition): Interpretation of Updated Key Points. Infect. Dis. Immun. *1*, 17–19. https://doi.org/10.1097/ID9.0000000000000002.
12. WHO Coronavirus (COVID-19) Dashboard. https://covid19.who.int.
13. Ginestra, J.C., Mitchell, O.J.L., Anesi, G.L., and Christie, J.D. (2022). COVID-19 Critical Illness: A Data-Driven Review. Annu. Rev. Med. *73*, 95–111. https://doi.org/10.1146/annurev-med-042420-110629.
14. Pagani, L., Chinello, C., Risca, G., Capitoli, G., Criscuolo, L., Lombardi, A., Ungaro, R., Mangioni, D., Piga, I., Muscatello, A., et al. (2023). Plasma Proteomic Variables Related to COVID-19 Severity: An Untargeted nLC-MS/MS Investigation. IJMS *24*, 3570. https://doi.org/10.3390/ijms24043570.
15. Wu, S., Xu, Y., Zhang, J., Ran, X., Jia, X., Wang, J., Sun, L., Yang, H., Li, Y., Fu, B., et al. (2022). Longitudinal Serum Proteome Characterization of COVID-19 Patients With Different Severities Revealed Potential Therapeutic Strategies. Front. Immunol. *13*, 893943. https://doi.org/10.3389/fimmu.2022.893943.
16. Ceballos, F.C., Virseda-Berdices, A., Resino, S., Ryan, P., Martínez-González, O., Peréz-García, F., Martin-Vicente, M., Brochado-Kith, O., Blancas, R., Bartolome-Sánchez, S., et al. (2022). Metabolic Profiling at COVID-19 Onset Shows Disease Severity and Sex-Specific Dysregulation. Front. Immunol. *13*, 925558. https://doi.org/10.3389/fimmu.2022.925558.
17. Ye, Q., Wang, B., and Mao, J. (2020). The pathogenesis and treatment of the 'Cytokine Storm' in COVID-19. J. Infect. *80*, 607–613. https://doi.org/10.1016/j.jinf.2020.03.037.
18. Hu, B., Huang, S., and Yin, L. (2021). The cytokine storm and COVID-19. J. Med. Virol. *93*, 250–256. https://doi.org/10.1002/jmv.26232.
19. Prusinkiewicz, M.A., and Mymryk, J.S. (2019). Metabolic Reprogramming of the Host Cell by Human Adenovirus Infection. Viruses *11*, 141. https://doi.org/10.3390/v11020141.
20. Macallan, D. (2009). Infection and malnutrition. Medicine *37*, 525–528.
21. Palmer, C.S. (2022). Innate metabolic responses against viral infections. Nat. Metab. *4*, 1245–1259. https://doi.org/10.1038/s42255-022-00652-3.
22. Mohammed, Y., Goodlett, D.R., Cheng, M.P., Vinh, D.C., Lee, T.C., Mcgeer, A., Sweet, D., Tran, K., Lee, T., Murthy, S., et al. (2022). Longitudinal Plasma Proteomics Analysis Reveals Novel Candidate Biomarkers in Acute COVID-19. J. Proteome Res. *21*, 975–992. https://doi.org/10.1021/acs.jproteome.1c00863.
23. Nishibori, M. (2022). Novel aspects of sepsis pathophysiology: NETs, plasma glycoproteins, endotheliopathy and COVID-19. J. Pharmacol. Sci. *150*, 9–20. https://doi.org/10.1016/j.jphs.2022.06.001.
24. Gao, S., Wake, H., Sakaguchi, M., Wang, D., Takahashi, Y., Teshigawara, K., Zhong, H., Mori, S., Liu, K., Takahashi, H., and Nishibori, M. (2020). Histidine-Rich Glycoprotein Inhibits High-Mobility Group Box-1-Mediated Pathways in Vascular Endothelial Cells through CLEC-1A. iScience *23*, 101180. https://doi.org/10.1016/j.isci.2020.101180.
25. Pan, Y., Deng, L., Wang, H., He, K., and Xia, Q. (2022). Histidine-rich glycoprotein (HRGP): Pleiotropic and paradoxical effects on macrophage, tumor microenvironment, angiogenesis, and other physiological and pathological processes. Genes Dis. *9*, 381–392. https://doi.org/10.1016/j.gendis.2020.07.015.
26. Miesbach, W., and Makris, M. (2020). COVID-19: Coagulopathy, Risk of Thrombosis, and the Rationale for Anticoagulation. Clin. Appl. Thromb. Hemost. *26*. 1076029620938149. https://doi.org/10.1177/1076029620938149.
27. Chen, T.-H., Chang, C.-J., and Hung, P.-H. (2023). Possible Pathogenesis and Prevention of Long COVID: SARS-CoV-2-Induced Mitochondrial Disorder. IJMS *24*, 8034. https://doi.org/10.3390/ijms24098034.
28. Nishibori, M., and Stonestreet, B.S. (2021). Understanding of COVID-19 Pathology: Much More Attention to Plasma Proteins. Front. Immunol. *12*, 656099. https://doi.org/10.3389/fimmu.2021.656099.
29. Gao, S., Wake, H., Gao, Y., Wang, D., Mori, S., Liu, K., Teshigawara, K., Takahashi, H., and Nishibori, M. (2019). Histidine-rich glycoprotein ameliorates endothelial barrier dysfunction through regulation of NF-κB and MAPK signal pathway. Br. J. Pharmacol. *176*, 2808–2824. https://doi.org/10.1111/bph.14711.

30. Ceperuelo-Mallafré, V., Reverté, L., Peraire, J., Madeira, A., Maymó-Masip, E., López-Dupla, M., Gutierrez-Valencia, A., Ruiz-Mateos, E., Buzón, M.J., Jorba, R., et al. (2022). Circulating pyruvate is a potent prognostic marker for critical COVID-19 outcomes. Front. Immunol. *13*, 912579. https://doi.org/10.3389/fimmu.2022.912579.
31. Páez-Franco, J.C., Maravillas-Montero, J.L., Mejía-Domínguez, N.R., Torres-Ruiz, J., Tamez-Torres, K.M., Pérez-Fragoso, A., Germán-Acacio, J.M., Ponce-de-León, A., Gómez-Martín, D., and Ulloa-Aguirre, A. (2022). Metabolomics analysis identifies glutamic acid and cystine imbalances in COVID-19 patients without comorbid conditions. Implications on redox homeostasis and COVID-19 pathophysiology. PLoS One *17*, e0274910. https://doi.org/10.1371/journal.pone.0274910.
32. Yelamanchi, S.D., Jayaram, S., Thomas, J.K., Gundimeda, S., Khan, A.A., Singhal, A., Keshava Prasad, T.S., Pandey, A., Somani, B.L., and Gowda, H. (2016). A pathway map of glutamate metabolism. J. Cell Commun. Signal. *10*, 69–75. https://doi.org/10.1007/s12079-015-0315-5.
33. Newsholme, P., Lima, M.M.R., Procopio, J., Pithon-Curi, T.C., Doi, S.Q., Bazotte, R.B., and Curi, R. (2003). Glutamine and glutamate as vital metabolites. Braz. J. Med. Biol. Res. *36*, 153–163. https://doi.org/10.1590/S0100-879X2003000200002.
34. Agarwal, S., Kaur, S., Asuru, T.R., Joshi, G., Shrimali, N.M., Singh, A., Singh, O.N., Srivastva, P., Shrivastava, T., Vrati, S., et al. (2022). Dietary alpha-ketoglutarate inhibits SARS CoV-2 infection and rescues inflamed lungs to restore O 2 saturation by inhibiting pAkt. Clin. Transl. Med. *12*, e1041. https://doi.org/10.1002/ctm2.1041.
35. Shrimali, N.M., Agarwal, S., Kaur, S., Bhattacharya, S., Bhattacharyya, S., Prchal, J.T., and Guchhait, P. (2021). α-Ketoglutarate Inhibits Thrombosis and Inflammation by Prolyl Hydroxylase-2 Mediated Inactivation of Phospho-Akt. EBioMedicine *73*, 103672. https://doi.org/10.1016/j.ebiom.2021.103672.
36. Singh, B., Eshaghian, E., Chuang, J., and Covasa, M. (2022). Do Diet and Dietary Supplements Mitigate Clinical Outcomes in COVID-19? Nutrients *14*, 1909. https://doi.org/10.3390/nu14091909.
37. Lee, S.R., Roh, J.Y., Ryu, J., Shin, H.-J., and Hong, E.-J. (2022). Activation of TCA cycle restrains virus-metabolic hijacking and viral replication in mouse hepatitis virus-infected cells. Cell Biosci. *12*, 7. https://doi.org/10.1186/s13578-021-00740-z.
38. Alfarouk, K.O., Alhoufie, S.T.S., Hifny, A., Schwartz, L., Alqahtani, A.S., Ahmed, S.B.M., Alqahtani, A.M., Alqahtani, S.S., Muddathir, A.K., Ali, H., et al. (2021). Of mitochondrion and COVID-19. J. Enzyme Inhib. Med. Chem. *36*, 1258–1267. https://doi.org/10.1080/14756366.2021.1937144.
39. Chernyak, B.V., Popova, E.N., Prikhodko, A.S., Grebenchikov, O.A., Zinovkina, L.A., and Zinovkin, R.A. (2020). COVID-19 and Oxidative Stress. Biochemistry. *85*, 1543–1553. https://doi.org/10.1134/S0006297920120068.
40. Rees, C.A., Rostad, C.A., Mantus, G., Anderson, E.J., Chahroudi, A., Jaggi, P., Wrammert, J., Ochoa, J.B., Ochoa, A., Basu, R.K., et al. (2021). Altered amino acid profile in patients with SARS-CoV-2 infection. Proc. Natl. Acad. Sci. USA *118*. e2101708118. https://doi.org/10.1073/pnas.2101708118.
41. Barberis, E., Timo, S., Amede, E., Vanella, V.V., Puricelli, C., Cappellano, G., Raineri, D., Cittone, M.G., Rizzi, E., Pedrinelli, A.R., et al. (2020). Large-Scale Plasma Analysis Revealed New Mechanisms and Molecules Associated with the Host Response to SARS-CoV-2. IJMS *21*, 8623. https://doi.org/10.3390/ijms21228623.
42. Feng, M., and Zhang, H. (2022). Aminoacyl-tRNA Synthetase: A Non-Negligible Molecule in RNA Viral Infection. Viruses *14*, 613. https://doi.org/10.3390/v14030613.
43. Liebich, H.M., and Först, C. (1984). Hydroxycarboxylic and oxocarboxylic acids in urine:products from branched-chain amino acid degradation and from ketogenesis. J. Chromatogr. *309*, 225–242. https://doi.org/10.1016/0378-4347(84)80031-6.
44. Jia, H., Liu, C., Li, D., Huang, Q., Liu, D., Zhang, Y., Ye, C., Zhou, D., Wang, Y., Tan, Y., et al. (2022). Metabolomic analyses reveal new stage-specific features of COVID-19. Eur. Respir. J. *59*, 2100284. https://doi.org/10.1183/13993003.00284-2021.
45. Sindelar, M., Stancliffe, E., Schwaiger-Haber, M., Anbukumar, D.S., Albrecht, R.A., Liu, W.-C., Travis, K.A., García-Sastre, A., Shriver, L.P., and Patti, G.J. (2021). Longitudinal Metabolomics of Human Plasma Reveals Robust Prognostic Markers of COVID-19 Disease Severity (Infectious Diseases (Except HIV/AIDS)). https://doi.org/10.1101/2021.02.05.21251173.
46. Valdés, A., Moreno, L.O., Rello, S.R., Orduña, A., Bernardo, D., and Cifuentes, A. (2022). Metabolomics study of COVID-19 patients in four different clinical stages. Sci. Rep. *12*, 1650. https://doi.org/10.1038/s41598-022-05667-0.
47. Peng, Y., Wan, L., Fan, C., Zhang, P., Wang, X., Sun, J., Zhang, Y., Yan, Q., Gong, J., Yang, H., et al. (2020). Cholesterol Metabolism—Impacts on SARS-CoV-2 Infection Prognosis (Infectious Diseases (Except HIV/AIDS)). https://doi.org/10.1101/2020.04.16.20068528.
48. Tang, Y., Hu, L., Liu, Y., Zhou, B., Qin, X., Ye, J., Shen, M., Wu, Z., and Zhang, P. (2021). Possible mechanisms of cholesterol elevation aggravating. Int. J. Med. Sci. *18*, 3533–3543.
49. Kočar, E., Režen, T., and Rozman, D. (2021). Cholesterol, lipoproteins, and COVID-19: Basic concepts and clinical applications. Biochim. Biophys. Acta. Mol. Cell Biol. Lipids *1866*, 158849. https://doi.org/10.1016/j.bbalip.2020.158849.
50. Dai, J., Wang, H., Liao, Y., Tan, L., Sun, Y., Song, C., Liu, W., Qiu, X., and Ding, C. (2022). Coronavirus Infection and Cholesterol Metabolism. Front. Immunol. *13*, 791267. https://doi.org/10.3389/fimmu.2022.791267.
51. Tanner, J.E., and Alfieri, C. (2021). The Fatty Acid Lipid Metabolism Nexus in COVID-19. Viruses *13*, 90. https://doi.org/10.3390/v13010090.
52. Loosen, S.H., Jensen, B.-E.O., Tanislav, C., Luedde, T., Roderburg, C., and Kostev, K. (2022). Obesity and lipid metabolism disorders determine the risk for development of long COVID syndrome: a cross-sectional study from 50,402 COVID-19 patients. Infection *50*, 1165–1170. https://doi.org/10.1007/s15010-022-01784-0.
53. Voinsky, I., Baristaite, G., and Gurwitz, D. (2020). Effects of age and sex on recovery from COVID-19: Analysis of 5769 Israeli patients. J. Infect. *81*, e102–e103. https://doi.org/10.1016/j.jinf.2020.05.026.
54. Liu, B., Jayasundara, D., Pye, V., Dobbins, T., Dore, G.J., Matthews, G., Kaldor, J., and Spokes, P. (2021). Whole of population-based cohort study of recovery time from COVID-19 in New South Wales Australia. Lancet Reg. Health. West. Pac. *12*, 100193. https://doi.org/10.1016/j.lanwpc.2021.100193.
55. Aleem, A., Akbar Samad, A.B., and Vaqar, S. (2023). Emerging Variants of SARS-CoV-2 and Novel Therapeutics Against Coronavirus (COVID-19). StatPearls. In StatPearls Publishing (Treasure Island).
56. Re3data.Org (2012). GISAID. https://gisaid.org/hcov-19-variants-dashboard/.

STAR★METHODS

KEY RESOURCES TABLE

REAGENT or RESOURCE	SOURCE	IDENTIFIER
Biological samples		
Human blood plasma samples	Hospital Universitari Joan XXIII (Tarragona) and the Vall d'Hebron Hospital (Barcelona)	N/A
Chemicals, peptides, and recombinant proteins		
1.4-Dithiothreitol	Sigma-Aldrich	https://www.sigmaaldrich.com/ES/es/product/sial/d0632
Iodoacetamide	Sigma-Aldrich	https://www.sigmaaldrich.com/ES/es/product/sigma/i1149
Formic acid	Sigma-Aldrich	https://www.sigmaaldrich.com/ES/es/product/sial/33015m
Acetonitrile	Merck	https://www.sigmaaldrich.com/ES/es/product/mm/100029
Methanol	Merck	https://www.sigmaaldrich.com/ES/es/product/mm/106035
Succinic acid-d4	Sigma-Aldrich	https://www.sigmaaldrich.com/ES/es/product/aldrich/293075
Myristic acid-d27	Sigma-Aldrich	https://www.sigmaaldrich.com/ES/es/product/aldrich/366889
Glycerol-13C3	Cortecnet	https://cortecnet.com/glycerol-13c3.html
D-glucose-13C6	Cortecnet	https://cortecnet.com/d-glucose-13c6.html
Methoxyamine hydrochloride	Sigma-Aldrich	https://www.sigmaaldrich.com/ES/es/product/aldrich/226904
MSTFA +1% TMCS	Thermo Scientific	https://www.thermofisher.com/order/catalog/product/TS-48915?SID=srch-hj-TS-48915
Chloroform	Sigma-Aldrich	https://www.sigmaaldrich.com/ES/es/product/sial/32211m
NaCl	Sigma-Aldrich	https://www.sigmaaldrich.com/ES/es/product/sial/s7653
Methyl-tert-butyl ether	Sigma-Aldrich	https://www.sigmaaldrich.com/ES/es/product/sigald/34875
2-propanol	Merck	https://www.sigmaaldrich.com/ES/es/product/mm/101040
Ammonium formate	Sigma-Aldrich	https://www.sigmaaldrich.com/ES/es/product/sigma/78314
Formic acid	Fisher Scientific	https://www.fishersci.es/shop/products/formic-acid-99-0-optima-lc-ms-grade-fisher-chemical/10596814?searchHijack=true&searchTerm=A117-50&searchType=RAPID&matchedCatNo=A117-50
Critical commercial assays		
Human-7 Multiple Affinity Removal Spin (MARS)	Agilent Technologies	https://www.agilent.com/en/product/biopharma-hplc-analysis/abundant-protein-depletion/multiple-affinity-removal-spin-cartridge-human-7
Pierce™ Trypsin/Lys-C Protease Mix, MS Grade	Thermo Fisher Scientific	https://www.thermofisher.com/order/catalog/product/es/es/A41007
TMT 11-plex labelling	Thermo Fisher Scientific	https://www.thermofisher.com/order/catalog/product/A34808
Lipidomic SPLASH	Avanti Lipids, INC	https://avantilipids.com/product/330707
Software and algorithms		
MetaboAnalyst 5.0	MetaboAnalyst	https://www.metaboanalyst.ca/
SPSS statistics 21.0	IBM Corporation	http://www.spss.com.hk/software/statistics/
GraphPad Prism 9.0	GraphPad	https://www.graphpad.com/
String 11.5	STRING CONSORTIUM 2023	https://string-db.org/
Proteome Discoverer v.1.4.0.288	Thermo Fisher Scientific	https://www.thermofisher.com/es
Mascot search engine v.2.5	Matrix Science	https://www.matrixscience.com/

RESOURCE AVAILABILITY

Lead contact

Further information and requests for resources and reagents should be directed to and will be fulfilled by the Lead Contact, Anna Rull (anna.rull@iispv.cat).

Materials availability

This study did not generate new unique reagents.

Data and code availability

Any additional information required to reanalyze the data reported in this paper is available from the lead contact upon request.

EXPERIMENTAL MODEL AND SUBJECT DETAILS

Study participants and data collection

This longitudinal COVID-19 cohort comprised 103 patients with SARS-CoV-2 infection confirmed by polymerase chain reaction (PCR) within the first 21 days of infection. All patients were recruited between March 2020 and February 2021 (from the first to the third waves) at the Hospital Universitari Joan XXIII (Tarragona) and the Vall d'Hebron Hospital (Barcelona). Although the SARS-CoV-2 strains were not identified in this study, Alpha (lineage 74 B.1.1.7), Beta (lineage B.1.351) and Delta (lineage B.1.617.2) strains were the predominant circulating variants during this period.[55,56] These patients were selected from a previous cohort[10] due to sampling at two time points: at the time of admission (acute phase) and after 4 to 8 weeks (recovery phase). None of the patients enrolled in the present study had received the SARS-CoV-2 vaccine at the time of blood sampling. According to the inclusion criteria described in "Diagnosis and Treatment Protocol for COVID-19 Patients" (version 8 trial),[11] COVID-19 patients were classified into three groups based on disease severity, namely, mild (n=40), severe (n=34) and critical (n=29) (Figure 1), as previously described.[10] Additionally, to determine severity biomarkers, the severe and critical groups were grouped into a single group named unfavourable group. The sample size was based on the availability of the samples. All information was collected and stored in a database specially designed for this purpose. The aforementioned database contained data regarding hospitalization, such as the symptoms presented at the time of admission, radiological findings, pneumonia degree, oxygen therapy needed, medical treatment received, demographic data and previous diseases of interest.

Ethics

Protocols were carried out in accordance with the recommendations of the Ethical and Scientific Committees from each participating institution and were approved by the Committee for Ethical Clinical Research following the rules of Good Clinical Practice from the IISPV (079/2020, CEIm IISPV) and from the Vall d'Hebron Hospital (PR(AG)192/2020). The CEIm IISPV is an independent committee made up of health and non-health professionals that supervise the correct compliance of the ethical principles governing clinical trials and research projects that are performed in our environment, specifically in their methodology, ethics, and laws. All subjects or their relatives gave written informed consent in accordance with the Declaration of Helsinki.

METHOD DETAILS

Sample recruitment

The blood sample was processed to obtain serum for used in the omics analysis. The sampling protocol performed included clinical evaluation, blood cell count, and standard biochemical parameters at baseline and after 4 to 8 weeks. Serum samples were stored at -80°C at Biobank—Institut d'Investigació Sanitària Pere Virgili (IISPV) facilities until used for omics analysis.

Proteomic analysis

Before proteomic analysis, the depletion of the seven most abundant plasma proteins (Albumin, IgG, antitrypsin, IgA, transferrin, haptoglobin and fibrinogen) was performed with the Human-7 Multiple Affinity Removal Spin (MARS) cartridges from Agilent Technologies following manufacturer's protocol. Thirty (30) μg of depleted protein were reduced with 4 mM 1.4-Dithiothreitol for 1h at 37°C and alkylated with 8 mM iodoacetamide for 30 min at 25°C in the dark. Afterwards, samples were overnight digested (pH 8.0, 37°C) with sequencing-grade Trypsin/Lys-C Protease Mix (ThermoFisher Scientific, CA, USA) at enzyme:protein ratio of 1:50. Digestion was quenched by acidification with 1% (v/v) formic acid and peptides were desalted on Oasis HLB SPE column (Waters, Massachusetts, USA) before TMT 11-plex labelling (Thermo Fisher Scientific, CA, USA) following manufacturer instructions. To normalize all samples in the study along the different TMT-multiplexed batches used, a pool containing all the samples was labelled with TMT-126 tag and included in each TMT. The different TMT 11-plex batches were desalted on Oasis HLB SPE columns before the nanoLC-MS analysis. Labelled and multiplexed peptides were loaded on a trap nano-column (100 μm I.D.; 2cm length; 5μm particle diameter, ThermoFisher Scientific, CA, USA) and separated onto a C18 reversed phase (RP) nano-column (75μm I.D.; 15cm length; 3μm particle diameter, Nikkyo Technos Co. LTD, Japan) on an EASY-II nanoLC from Thermo Fisher. The chromatographic separation was performed with a minutes (min) gradient using Milli-Q water (0.1% formic acid) and acetonitrile (0.1% formic acid) as mobile phase at a flow rate of 300 nL/min. Each TMT-plex was analysed twice to increase the peptide and protein

coverage. Mass spectrometry analyses were performed on an LTQ-Orbitrap Velos Pro from ThermoFisher by an enhanced FT-resolution MS spectrum 4 (R=30,000 FHMW) followed by a data-dependent FT-MS/MS acquisition (R=15,000 FHMW, 40% HCD) from the most intense ten parent ions with a charge state rejection of one and dynamic exclusion of 0.5 minutes. Protein identification and quantification were performed on Proteome Discoverer software v.1.4.0.288 (ThermoFisher Scientific, CA, USA) by Multidimensional Protein Identification Technology (MudPIT) combining the two raw data files obtained from each sample. For protein identification, all MS and MS/MS spectra were analyzed using Mascot search engine (v.2.5) combing Homo sapiens (74449 entries) and contaminants (247 entries) databases. Two missed cleavages were allowed and an error of 0.02 Da for FT-MS/MS fragmentation mass and 10.0 ppm for a FT-MS parent ion mass were allowed. TMT-10plex was set as quantification modification and oxidation of methionine and acetylation of N-termini were set as dynamic modifications, whereas carbamidomethylation of cysteine was set as static modifications. The false discovery rate (FDR) and protein probabilities were calculated by Percolator. For protein quantification, the ratios between each TMT-label against-TMT label were used and quantification results were normalized based on the protein median.

Metabolomic analysis

For metabolomics analysis, a protein precipitation extraction was performed by adding eight volumes of methanol:water (8:2) containing internal standard mixture (succinic acid-d4, myristic acid-d27, glycerol-13C3 and D-glucose-13C6) to serum samples. Samples were mixed and incubated at 4°C for 10 minutes, centrifuged at 15,000 rpm and the supernatant was evaporated to dryness before compound derivatization (methoxyamine hydrochloride and MSTFA +1% TMCS). Samples were analyzed on a 7200 GC-qTOF from Agilent Technologies (Santa Clara, CA, USA). The chromatographic separation was based on Fiehn Method, using a J&W Scientific HP5-MS (30 m x 0.25 mm i.d., 0.25 μm film capillary column and helium as carrier gas using an oven program from 60°C to 325°C. Ionization was done by electronic impact (EI), with electron energy of 70eV and operated in full scan mode, recording data in a range between 35 and 700 m/z at a scan rate of 5 spec/s. Targeted compounds from central carbon metabolism were identified using pure standards, in addition, screening for the identification of more metabolites was performed by matching their EI mass spectrum and retention time to the metabolomic Fiehn library (from Agilent) which contains more than 1,400 metabolites. After putative identification of metabolites, these were semi-quantified in terms of internal standard response ratio.

Lipidomic analysis

For the extraction of hydrophobic lipids, liquid-liquid extraction with chloroform:methanol (2:1) based on the Folch procedure was performed by adding four volumes of chloroform:methanol (2:1) containing internal standard mixture (Lipidomic SPLASH®) to serum (20 μL). Then, the samples were mixed and incubated at -20°C for 30 min. Afterwards, water with NaCl (0.8 %) was added and the mixture was centrifuged at 15,000 rpm. The lower phase was recovered, evaporated to dryness and reconstituted with methanol:methyl-tert-butyl ether (9:1). Samples were analyzed on a 1290 Infinity UHPLC coupled to a 6550 qTOF mass spectrometer from Agilent Technologies (Santa Clara, CA, USA). The chromatographic separation consists of an elution with a ternary mobile phase containing water, methanol and 2-propanol with 10mM ammonium formate and 0.1% formic acid. The stationary phase was a C18 column (Kinetex EVO C18 Column, 2.6 μm, 2.1 mm X 100 mm) that allows the sequential elution of the more hydrophobic lipids such as lysophospholipids, sphingomyelins, phospholipids, diglycerides, cholesteryl esters and triglycerides, among others. The identification of lipid species was performed by matching their accurate mass and tandem mass spectrum, when available, to Metlin-PCDL from Agilent containing more than 40,000 metabolites and lipids. Chromatographic behaviour of pure standards for each family and bibliographic information was used to ensure their putative identification. After putative identification of lipids, these were semi-quantified in terms of internal standard response ratio using one internal standard for each lipid family.

QUANTIFICATION AND STATISTICAL ANALYSIS

Statistical analysis

Before the statistical analyses, the distribution and homogeneity of the variances were tested using a Kolmogorov–Smirnov test. Global significance regardless of the disease severity and qualitative variables such as sex, symptoms, comorbidities and clinical treatments was calculated with the $\chi 2$ test for categorical data. To carry out the analysis of the evolution of the omics profile, the fold change was calculated, and the Wilcoxon test for paired samples was used to detect significant changes. The volcano plot was generated using MetaboAnalyst 5.0 software. The recovery phase data were normalized by calculating the ratio between the data at 4 to 8 weeks divided by the data at the time of admission (baseline). The Kruskal–Wallis and Mann–Whitney tests were employed to assess significant differences between severity groups. The protein network was constructed with the online String software (version 11.5). Random forest analyses were performed to determine the proteins, lipids and metabolites with higher accuracy for classifying patients according to disease severity. Pathway enrichment and joint-pathway analyses were conducted to explore the association of the significant biomolecules, COVID-19 severity and related metabolomic pathways. Random forest, enrichment and joint-pathway analyses were performed using MetaboAnalyst 5.0 software. Venn diagrams were performed by R Studio using the VennDiagram library. Binary logistic regression models and receiver operating characteristic (ROC) curves were generated by IBM SPSS Statistics 21.0 (IBM Corp. Released 2012. IBM SPSS Statistics for Windows, Version 21.0. Armonk, NY: IBM Corp.) to evaluate the potential accuracy of the selected biomarkers for predicting

COVID-19 severity. Logistic regression analyses were performed to evaluate the potential accuracy of different candidates, and to optimize all the model components, stepwise variable selection was used. Correlations between qualitative variables, comorbidities and levels of selected biomarkers were calculated using the point-biserial correlation coefficient, and graphical representations were generated with GraphPad Prism software (version 9.0, GraphPad Inc., San Diego, CA). Complex and detailed figures were created with BioRender.com. The results were considered statistically significant at $P < 0.05$.